Vanadyl as a Spectroscopic Probe of Tunable Ligand Donor Strength in Bimetallic Complexes

Claire M. Dopp,[a] *Riddhi R. Golwankar,*[a] *Shaun R. Kelsey,*[a] *Alexander N. Erickson,*[b] *Justin T. Douglas,*[c] *and James D. Blakemore*[a,*]

[a] Department of Chemistry, University of Kansas,

1567 Irving Hill Rd, Lawrence, Kansas 66045, United States

[b] Department of Chemistry, University of Memphis,

3744 Walker Ave, Memphis, Tennessee 38152, United States

[c] Nuclear Magnetic Resonance Laboratory, Molecular Structures Group,

University of Kansas, 2034 Becker Dr, Lawrence, Kansas 66047, United States

* To whom correspondence should be addressed.

E-mail: blakemore@ku.edu. Phone: +1 (785) 864-3019

ABSTRACT. Incorporation of secondary metal ions into heterobimetallic complexes has emerged as an attractive strategy for rational tuning of compounds' properties and reactivity, but direct solution-phase spectroscopic interrogation of tuning effects has received less attention than it deserves. Here, we report assembly and study of a series of heterobimetallic complexes containing the vanadyl ion, $[VO]^{2+}$, paired with mono-valent cations (Cs^+, Rb^+, K^+, Na^+, and Li^+)

or a di-valent cation (Ca^{2+}). These complexes, which can be isolated in pure form or generated *in situ* from a common monometallic vanadyl-containing precursor, enable experimental spectroscopic quantification of the influence of the incorporated cations on the properties of the vanadyl moiety. The data reveal systematic shifts in the V–O stretching frequency and isotropic hyperfine coupling constant for the vanadium center in the complexes. These shifts can be interpreted as charge density effects parametrized through the Lewis acidities of the cations, suggesting broad potential for the vanadyl ion to serve as a spectroscopic probe in multimetallic species.

INTRODUCTION

The coordination chemistry of multimetallic complexes has become a premiere research topic in inorganic chemistry, in part due to the recognized ability of effectively Lewis acidic metals to rationally tune their parent metal complexes upon incorporation. Multimetallic compounds and complexes often afford access to structural and chemical properties that are inaccessible in their homometallic analogues, making them attractive for development as catalysts and model systems. Progress in understanding the roles that secondary metal cations can play in those multimetallic systems has come from studies of molecular model compounds, particularly those based on first-row transition metals.[1,2]

As charged species that do not readily engage in significant covalent bonding, electropositive metal cations such as Na^{+}, Ca^{2+}, and Y^{3+} have been envisioned to exert electrostatic effects in multimetallic complexes, giving rise to changes in chemical reactivity,[3] catalytic behavior,[4,5,6] and in many cases, electrochemical reduction potentials.[7,8] These effects have been parametrized through a variety of descriptors, including the cations' charges, their ionic radii,[9] or their

effective Lewis acidities, as estimated from the pK_a values of their corresponding metal aqua complexes.[10] Other parametrizations based on spectroscopic measurements have also been proposed because of the influence that solvent effects and metal ion speciation can exert over quantitative descriptors. For example, Fukuzumi and co-workers have explored systematic differences among cations with electron paramagnetic resonance (EPR) experiments on *in situ* generated superoxide species,[11] Caputo and co-workers have developed an approach to measuring Lewis acidity with fluorescence measurements,[12] and our group has been examining use of phosphine oxide probes and ^{31}P nuclear magnetic resonance (NMR) methods to quantify the properties of diamagnetic cations.[13] In all these cases, there is motivation to pursue a quantitative measure of the tendency of a given chemical species (*e.g.*, electropositive metal cation) to serve effectively as a Lewis acid. Such behavior can be thought to arise from the induced shift in charge density distribution that results from interaction of a given Lewis acid with a molecule of interest.

Synthetic methods have remained elusive, however, for generation of heterobimetallic complexes featuring spectroscopically addressable moieties suited for study in the presence of closely-spaced metal cations and in the solution phase. Spectroscopy is a particularly powerful tool for observing the chemical properties of multimetallic species, and has been deployed for this purpose in many notable cases.[14] We envisioned that taking a hybrid approach could be fruitful for understanding the specific changes induced by installation of a tunable series of electropositive metal cations; in particular, two different metals could be held in close proximity by a tailored ligand, and a moiety could be installed in the complexes that could serve as a probe of electronic and magnetic environment. The ligand frameworks developed by Reinhoudt and co-workers[15] and elaborated upon by Vigato and co-workers[16] that feature [N_2,O_2] and [O_6]

binding sites seemed ideal for this purpose, as they enable stable binding of cations in solution.[17,18] Thus, we targeted installation of the vanadyl ion, $[VO]^{2+}$ or oxovanadium(IV), for incorporation into heterobimetallic complexes as this species is chemically robust[19] (attributable to the formal V–O triple bond),[20] features a well-resolved V–O stretching frequency near 990 cm^{-1}, and its paramagnetic nature, which gives rise to a distinctive eight-line electron paramagnetic resonance (EPR) spectrum for the $S = 1/2$ and $I = 7/2$ spin system.[21] Such properties could enable use of vanadyl as a spectroscopically addressable probe of ligand field strength, affording new insights into the properties of heterobimetallic complexes.

Here, we report the assembly of a series of heterobimetallic complexes that pair the vanadyl ion with a secondary electropositive metal cation (Cs^+, Rb^+, K^+, Na^+, Li^+ or Ca^{2+}) and solution-phase spectroscopic measurements which quantify the influence of the secondary metal cations on the vanadyl core. The vanadyl ion, $[VO]^{2+}$, appears robust in these systems, and the complexes themselves can be either *i)* isolated and characterized as powdered samples or *ii)* prepared *in situ* and used directly for solution-phase spectroscopic investigations. Findings from electronic absorption, infrared and EPR spectroscopies enable quantification of a decrease in ligand donor power upon incorporation of more effective Lewis acids. Taken together, the results described here reveal the power of incorporating a spectroscopic probe into heterobimetallic complexes and suggest vanadyl could be broadly useful for this purpose.

RESULTS

Synthesis of the heterobimetallic vanadyl complexes was accomplished with a monometallic precursor denoted **[VO]** (see Figure 1, panel (a)). **[VO]** was prepared from **[H_2,Ba]** by stirring in an excess of guanidinium sulfate in chloroform (resulting in extraction of Ba^{2+})[18,15] followed by

addition of 1 equiv. of $VO(acac)_2$ (where acac = acetylacetonate)[22] along with a few drops of triethylamine. **[VO]** was isolated with our procedures (see Experimental Section) in good yield (76%) as a green powder, and is soluble in acetonitrile (CH_3CN) and tetrahydrofuran. Due to the paramagnetic nature of this complex, the ^1H NMR spectrum of **[VO]** features broad, shifted resonances (see SI, Figure S1); a lack of typical peaks for diamagnetic species or impurities, however, confirmed successful isolation of the desired compound. Elemental analysis and structural data from X-ray diffraction (XRD) analysis (see Figure 1, panel (b) for structure) also confirmed the formulation of **[VO]**, including the presence of the free crown-ether-like [O_6] site that appears poised for binding of secondary metal cations.

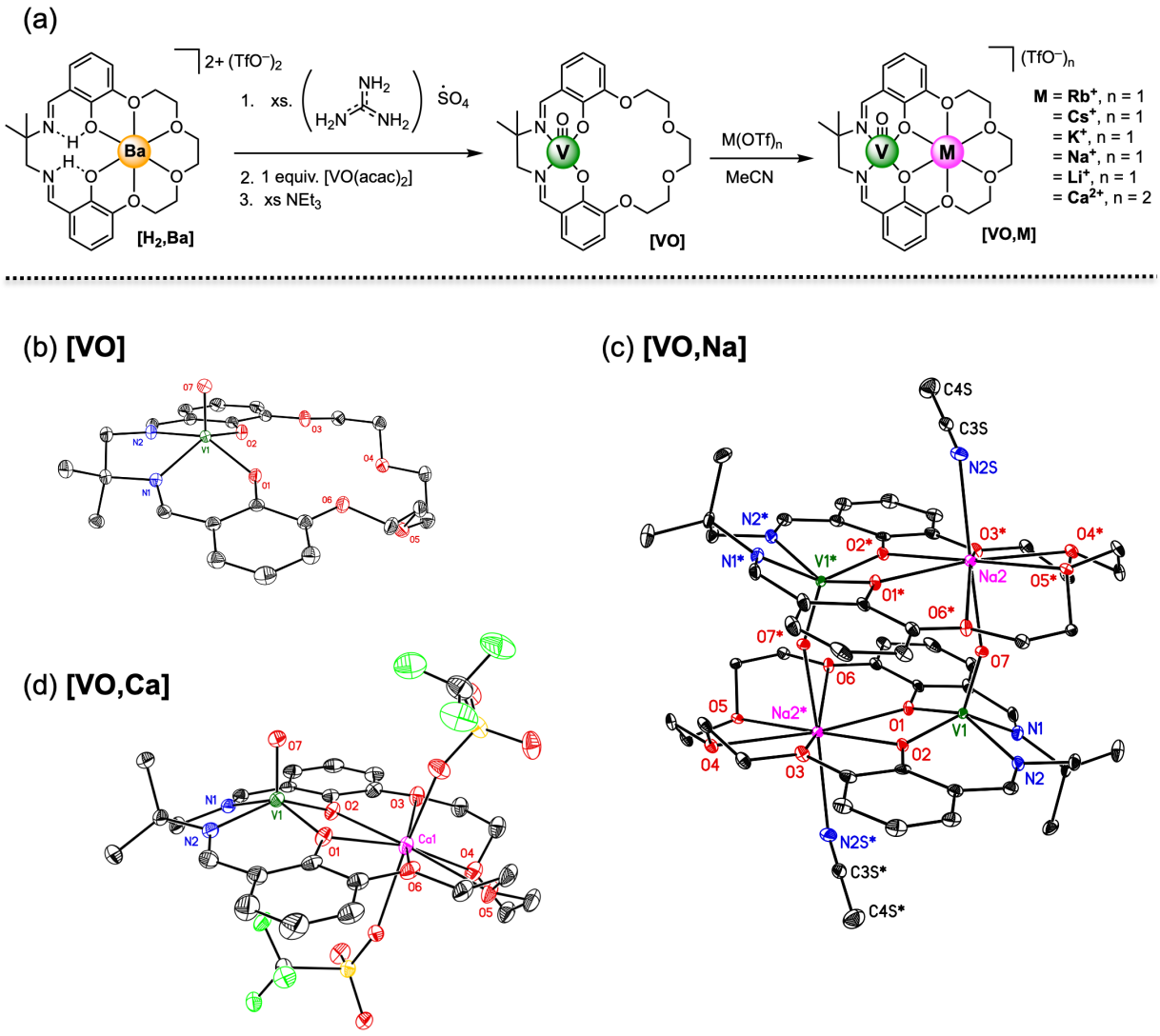

Figure 1. (a) Synthetic strategy for preparation of heterobimetallic vanadyl complexes. (b) Solid-state structure of **[VO]** from XRD; displacement ellipsoids shown at the 50% probability level; two outer-sphere co-crystallized acetonitrile solvent molecules are omitted for clarity. (c) Solid-state structure of **[VO,Na]** from XRD; outer-sphere triflate counter-anions and a second dimeric unit composed of the heterobimetallic species displaying disorder are omitted for clarity; displacement ellipsoids shown at the 50% probability level. (d) Solid-state structure of **[VO,Ca]** from XRD; displacement ellipsoids shown at the 20% probability level; a co-crystallized

molecule of outer-sphere co-crystallized acetonitrile solvent and disorder associated with the structure are omitted for clarity. All H-atoms omitted for clarity.

To demonstrate the ability of **[VO]** to cleanly incorporate secondary metal cations, **[VO,Cs]**, **[VO,Na]**, and **[VO,Ca]** were also isolated and fully characterized (see Experimental Section for details). These compounds could be readily prepared by addition of 1 equiv. of the corresponding triflate salts of the desired secondary metal cations (Cs^+, Na^+, and Ca^{2+}) to solutions of **[VO]** in CH_3CN. The heterobimetallic species were isolated in good yields (>85%) in each case, in line with clean reactivity in solution. **[VO,Cs]**, **[VO,Na]**, and **[VO,Ca]** were fully characterized, including by elemental analysis, while solid-state structural data from XRD for **[VO,Na]**, and **[VO,Ca]** confirmed the ability of the pendant crown-ether-like [O_6] site in **[VO]** to effectively bind both monovalent and divalent secondary metals in the solid state.

Single-crystals of **[VO]**, **[VO,Na]**, and **[VO,Ca]** suitable for XRD analysis were grown by vapor diffusion of diethyl ether into CH_3CN in all three cases. (See Table 1 for metrical data from XRD and SI pp. S33-S49 for details.) The vanadyl moiety adopts a square pyramidal geometry in all three complexes, coordinating to the [N_2,O_2] site as the base of the square pyramid and not interacting directly with atoms of the crown-ether-like [O_6] site. **[VO]** is overall neutral, and crystallized with two outer-sphere acetonitrile molecules in our structure; these data confirm that the [O_6] site is open and available to bind secondary metal cations. The Na^+ and Ca^{2+} cations occupy the [O_6] site in the structures of **[VO,Na]** and **[VO,Ca]** as expected, and the cations are both eight-coordinate in the solid-state data. In addition to the six oxygen donors, Ca^{2+} is ligated by two inner-sphere κ^1 triflate counter-anions while Na^+ is ligated by one inner-

sphere acetonitrile molecule and the oxo of a nearby vanadyl moiety, resulting in the triflate counter-anions being found in the outer sphere. **[VO,Na]** was revealed to be a dimer in the solid state data, driven by a long, weak Na•••O_{oxo} interaction of ca. 2.304(3) Å. The distance between the phenoxide donors ($d_{O\cdots O}$) decreases upon incorporation of the secondary metal cations (see Table 1), with the smaller values of $d_{O\cdots O}$ and the V•••M distance ($d_{V\cdots M}$) being associated with the more Lewis acidic calcium ion. Most notably, however, the V–O_{oxo} bond undergoes a marginally significant contraction upon binding of Na^+ or Ca^{2+}, giving data for this bond distance that decrease in the order **[VO]** > **[VO,Na]** > **[VO,Ca]**. This observation suggests that the properties of the vanadyl core are indeed measurably perturbed upon incorporation of more strongly Lewis acidic cations into **[VO]**, and thus we turned to our solution phase spectroscopic investigations to provide further quantitative evidence for such perturbations.

Table 1. Comparison of structural parameters from X-ray diffraction analysis

Compound	**[VO]**	**[VO,Na]** [c]	**[VO,Ca]**
pK_a of [**M**$(H_2O)_m$]$^{n+}$ [a]	-	14.8	12.6
Ionic radius of **M** [b]	-	1.18	1.12
C.N. of M^{n+}	-	8	8
$d_{V\text{-}Oxo}$ (Å)	1.605(1)	1.597(3)	1.583(3)
$d_{V\cdots M}$ (Å)	-	3.530(2)	3.524(1)
$d_{O\cdots O}$ (Å)	2.650(2)	2.604(4)	2.583(5)

[a] From reference 10. [b] From reference 9. [c] Average values of the interatomic distances for **[VO,Na]** were calculated as the arithmetic mean of the values for the two independent molecular species present in the asymmetric unit. The stated e.s.d.'s on these distances are taken as the larger of the original values in the refined data for the independent molecular species.

We first applied electronic absorption spectroscopy to understand if the full range of heterobimetallic complexes in our study, pairing vanadyl with Cs^+, Rb^+, K^+, Na^+, Li^+, and Ca^{2+}, could be assembled *in situ* in acetonitrile solution for spectroscopic studies, rather than studied by bulk isolation and solid-state characterization as has often been pursued more commonly in the field. Therefore, we prepared 1:1 vanadium:**M** solutions over a vanadium concentration of 0.025 to 0.5 mM, and measured these solutions' UV-visible spectra under inert atmosphere in our glove box. Two notable absorption bands were measured for the starting **[VO]** complex, and these bands were also observed for the heterobimetallic species, albeit shifted to higher energies in all cases (see SI, Figures S9-S20 for spectra and details). The higher energy absorption band was found for **[VO]** at λ_{max} = 386 nm, and was assigned as a charge-transfer (CT) band on the basis of its intense molar absorptivity (ε = 4,500 M^{-1} cm^{-1}). The second notable absorption band was found for **[VO]** at 593 nm, and on the basis of its position[23] as well as lower intensity ($\varepsilon \approx$ 130 M^{-1} cm^{-1}),[20] we assigned this as a d-d band associated with the vanadyl moiety.

In all cases, the UV-visible spectra revealed linear relationships between concentration and the values of absorption at the unique λ_{max} values for each compound (in accord with the Beer-Lambert law), as well as invariant λ_{max} values when compared across secondary metal cation concentrations (see SI, Figure S16). We thus conclude that the heterobimetallic species are stable in solution in each case, in line with the proven ability of crown-ether-like sites in Reinhoudt-type macrocycles to tightly bind secondary cations.

Plotting the energies of both the notable absorption bands as a function of Lewis acidity (parametrized by pK_a values as described above) results in linear trends in both cases, with the exception of the data for **[VO,Li]** (see SI, Figures S18 and S20). Looking to the literature, there

is an established preference of Li^+ to bind in smaller crown ethers such as 15-crown-5 as well as a propensity for Li^+ to directly bind to and/or interact with the terminal oxo ligands of both vanadyl as well as uranyl and other actinyl cations.[24,25] This suggests that the size mismatch between our 18-crown-6-like site and the presence of a possible secondary site for Li^+ (to bind to the vanadyl ion directly) contributes to a different solution-phase placement of Li^+ than the other cations in our series of **[VO,M]** complexes. Consequently, we have not considered the data for **[VO,Li]** in our exploration of spectroscopic trends among our series, due to the likely direct interaction between the Li^+ cation and the vanadyl moiety through a bridging oxo interaction. However, all data for **[VO,Li]** were tabulated and are included here for comparison to the data on the other complexes which appear to behave similarly, as suggested by the XRD data and systematic spectroscopic features.

With all this in mind, the dependence of the CT band energy for the adducts of Cs^+, Rb^+, K^+, Na^+, and Ca^{2+} on Lewis acidity was found to be −30±5 meV/pK_a, whereas the value was found to be −50±10 meV/pK_a for the d-d transition. The values of these slopes are in the neighborhood of prior dependences that we have measured in related Ni,[17] Pd,[18] and uranyl[26] heterobimetallic complexes (–46±5, –45±3, and –22±1, respectively), in line with the similar structure of the ligands used in each case. The use of vanadyl here, however, enabled us to measure the dependence of its d-d energy on the Lewis acidity of nearby cations; the higher dependence of this energy on Lewis acidity suggests, at least, that the close proximity of the vanadium(IV) center to the site for binding of the secondary metal cations results in a significantly greater sensitivity to the influence of these cations in comparison to their influence over the CT band energies in the same compounds. For the **[VO,Li]** complex, we note that the UV-visible data qualitatively resemble those for the other cation adducts, with blue shifts noted for the key

absorption bands; however, the shifts for **[VO,Li]** are more modest than what would be expected on the basis of Lewis acidity, suggesting that the cation interacts with the parent **[VO]** complex at multiple sites or that equilibria between binding sites on the complex impact this species' behavior.

With these results in hand, we next moved to directly interrogate the vibrational properties of the vanadyl core of our heterobimetallic complexes with infrared (IR) spectroscopy. The solution phase IR spectrum of **[VO]** collected in CH_3CN exhibits a feature at 989 cm^{-1} which can be assigned on the basis of prior work with vanadyl complexes[27] to be associated with the asymmetric stretch of the V–O moiety (see Figure 2, black line, and Figure S21 in SI). A shift of this V–O stretching frequency to higher wavenumbers was observed upon incorporation of more Lewis acidic cations to form the heterobimetallic complexes, with the greatest shift of 14 cm^{-1} being encountered in the case of **[VO,Ca]** (see Figure 2, Table 2, and SI Figures S22-S26 for full spectra). This observation is consistent with deformation of the electron density of phenoxide parentage in the heterobimetallic complexes, resulting in an attenuation of electron donation to the vanadyl moiety. The $V–O_{oxo}$ bond strengthens upon incorporation of secondary metal cations into **[VO]**, and we hypothesize that that this is due to a charge density effect induced by the nearby secondary metal cations. The strength of the $V–O_{oxo}$ bond increases monotonically as the Lewis acidity of the secondary metal cations increases, indicating that this descriptor is appropriate for interpreting the observed spectroscopic changes (see SI, Figure S27). We also note here that infrared data could not be measured for **[VO,Li]** as preparation of concentrated samples of this compound resulted in precipitation of insoluble material, perhaps consistent with speciation of the Li^+ cations and/or binding outside of the crown-ether-like site of **[VO]**.

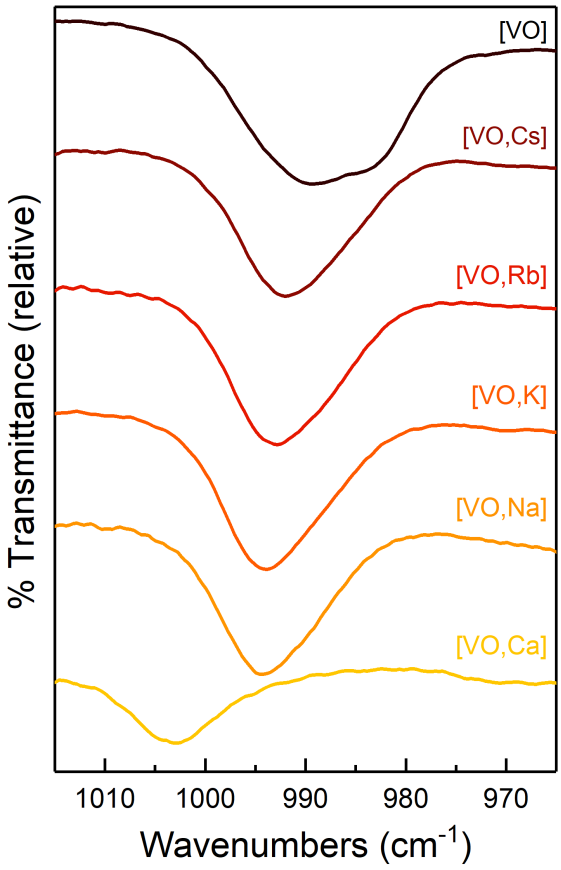

Figure 2. Infrared spectra for the **[VO,M]** complexes. Conditions: CH_3CN solvent; [VO] = 10 mM; KBr window cell.

Table 2. Comparison of quantitative data from infrared spectroscopy and fitted parameters from EPR analysis.

Compound	pK_a of $[\mathbf{M}(H_2O)_m]^{n+}$ [a]	ν_{V-O} (cm^{-1}) [b]	Δg [c]	A_{iso} (MHz) [d]	g_{avg} [e]
[VO]	-	991	0.395	271.9	1.9695
[VO,Cs]	16.34	992	0.398	274.0	1.9702
[VO,Rb]	16.29	993	0.399	274.9	1.9705
[VO,K]	16.06	994	0.401	275.9	1.9708
[VO,Na]	14.8	995	0.403	277.7	1.9713
[VO,Ca]	12.6	1003	0.407	280.1	1.9727
[VO,Li]	13.8	-	0.407	275.9	1.9719

[a] From reference 10. [b] Asymmetric $V–O_{oxo}$ stretching frequency. Error from triplicate runs (±1σ) was ±1 cm^{-1}. Measured at the transmittance minimum of the assigned peak. [c] Measured as the difference in *g* between the maxima of the derivative low-field and high-field features in the EPR spectra. (see SI, Figures S37). [d] Isotropic hyperfine coupling constant from fitting of spectral data. Error from triplicate runs (±1σ) was determined to be ±0.1 MHz.
[e] Average *g*-value from fitting of spectral data. Error from triplicate runs (±1σ) was determined to be ±0.001.

Further support for the hypothesis regarding attenuation of the phenoxide ligand donor strength comes from X-band electron paramagnetic resonance (EPR) spectra collected in CH_3CN solution at room temperature. As we desired to use CH_3CN as the solvent for this work, we prepared capillaries containing the heterobimetallic complexes in CH_3CN and loaded these into conventional quartz EPR tubes in our glovebox prior to transferring the sealed samples to the spectrometer for data collection. The spectra thus obtained (see Figure 3, solid lines) reveal a distinctive eight-line signal centered near $g = 2.0$ in each case, consistent with the formal +IV oxidation state and $S = 1/2$ configuration of the vanadyl ions in each heterobimetallic complex.[28]

However, there is a subtle but nonetheless measurable widening of the spectral profile when comparing the spectra of the heterobimetallic complexes to that of the **[VO]** precursor, consistent with an increase in apparent *g* anisotropy (Δg) that is driven by the incorporation of secondary metal cations (see Table 2).

Our vanadyl complexes are five-coordinate on the basis of the solid-state structures from XRD. The oxo ligand is typically used to define the *z*-direction of the coordination polyhedron in complexes of this type, and the strong interaction with this ligand has been found to give rise to large, approximately axial anisotropy in the hyperfine characteristics of the vanadyl ion. It is known that the identity of the four equatorial ligands can give rise to differences in hyperfine coupling constants in those *x* and *y* coordinates (A_x and A_y), and also that the identity or absence of a sixth ligand *trans* to the oxo group often results in little impact on the hyperfine characteristics of a given system. Our spectra fit well in the context of these prior findings,[28] although we note that the collection of our spectra in homogeneous, liquid solution and thus the individual contributions of $g_{\parallel}$ and $g_{\perp}$ are not directly observed in the spectral data due to the influence of tumbling in solution.

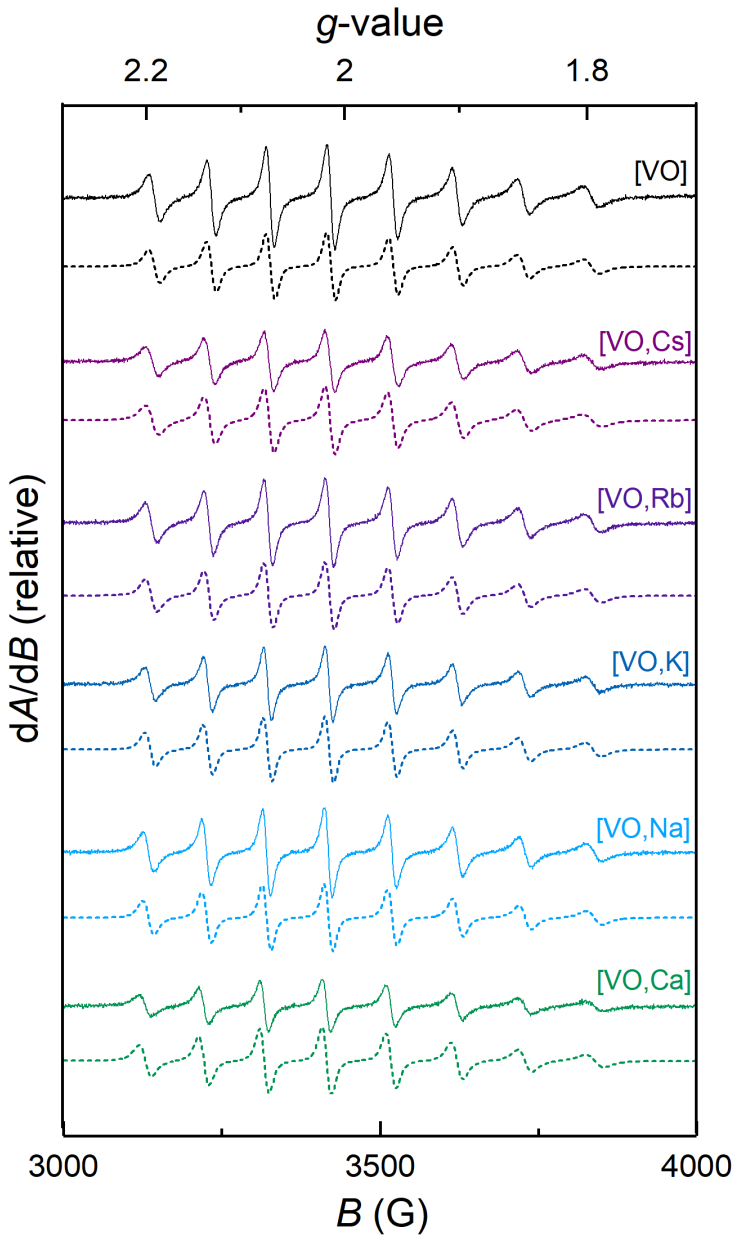

Figure 3. X-band EPR spectra of **[VO,M]** complexes in CH_3CN. Experimental data are given in the solid lines. [VO] was ca. 10^{-3} M in each case. (Conditions: T = 298 K; modulation amplitude = 4.0 G; time constant = 1.28 ms). Simulated spectra (EasySpin) are given in the dashed lines below each experimental spectrum.

In order to fully quantify the magnetic properties underlying our spectral data and any changes to them induced by the secondary metal cations, we turned to spectral simulation and fitting with the *garlic* function in the EasySpin package,[29] an approach which allowed us to extract the value of the isotropic hyperfine coupling constant (A_{iso}) for each complex, as well as the values of $g_{\parallel}$ and $g_{\perp}$ for the vandyl moiety in each complex (see SI, Figures S29-S39 for details).[30] In our simulations, the spectra could be modeled well with a single $S = ½$ radical species displaying axial symmetry, under conditions of free tumbling in solution. The EPR simulations reveal a distinctive increase in the value of A_{iso} for the vanadyl ion in the heterobimetallic complexes studied here (see Figure 4). This increase in hyperfine coupling constant gives rise to the noted anisotropic widening (or broadening) of the spectral profile described above, with the largest values being measured for the derivatives incorporating Na^+ and Ca^{2+}. Thus, as the Lewis acidity of the secondary metal cation increases, A_{iso} increases in our complexes.

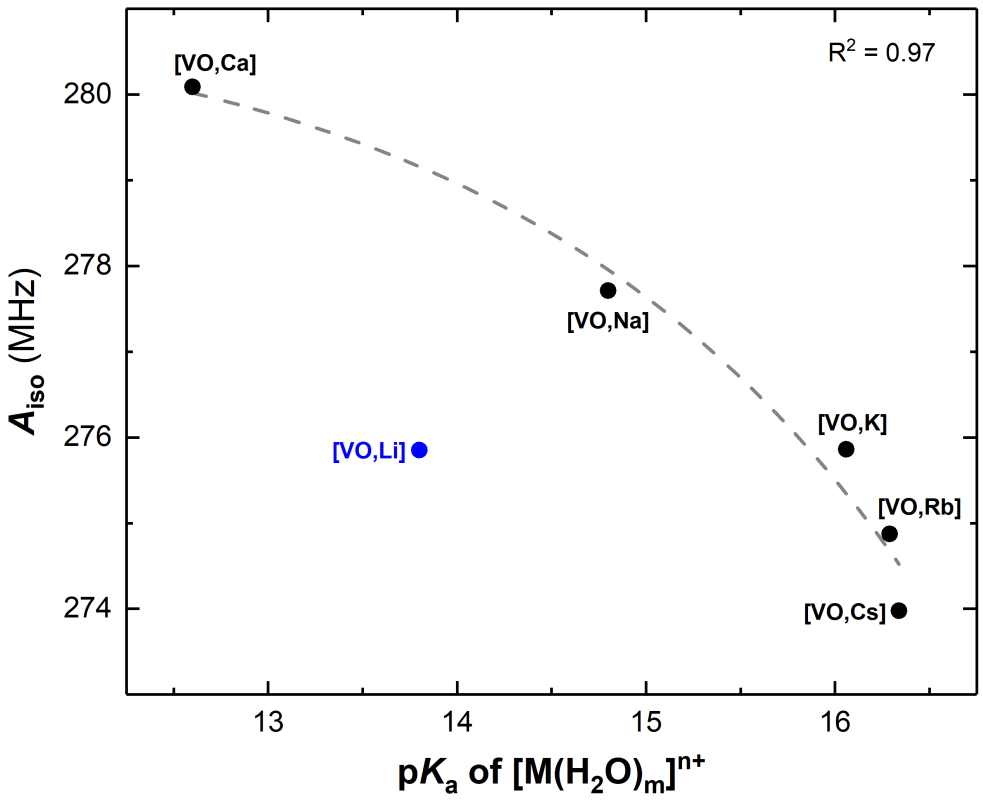

Figure 4. Plot of A_{iso} (MHz) for the **[VO,M]** complexes vs. pK_a of [**M**$(H_2O)_m]^{n+}$. The gray dashed line corresponds to an exponential fit of the data excluding the point for [**VO,Li]** and is intended as a guide to the eye for the monotonic relationship in the data.

Our approach of using the vanadyl ion as a spectroscopic probe or reporter in heterobimetallic complexes represents a strategy reminiscent of prior work from the field of the bioinorganic chemistry of vanadium-containing enzymes and proteins.[31,32] In particular, pioneering work from Wüthrich and co-workers[33] demonstrated that controlled substitution of the ligand environment around the vanadyl ion in protein matrices resulted in measurable changes in hyperfine coupling. The theory regarding vanadyl EPR spectra has evolved considerably over the years,[34,35] enabling

use of hyperfine coupling constants as a sensitive probe of electronic environment.[36] In particular, an additivity relationship has been developed which correlates the number and types of ligands present in the equatorial plane of the vanadyl ion to its spectral properties in a given system.[34] The maagnitudes of the hyperfine components are quite sensitive to the electron-donating ability of the equatorial ligands, and within this paradigm, EPR measurements carried out on biological systems with known (or presumed) identities have been useful for assigning the identity of coordinating ligands in vanadyl-containing biological systems.[37] In our family of complexes, this relationship appears to be manifest as a monotonic dependence of the A_{iso} values of the **[VO,M]** complexes on the pK_a values of the incorporated secondary metal cations (see Figure 4). This is consistent with the prior work on biological systems, in that weaker electron donors (e.g., oxides) generally result in narrower spectra and smaller A_{iso} values whereas stronger donors (e.g., sulfides) give larger A_{iso} values.[34,37] Thus, our EPR data reveal a quantitative measure of diminished electron donation from the bridging phenoxide ligands to the vanadium(IV) center in the vanadyl ion.

DISCUSSION

The relationship among the measured A_{iso} values when plotted as a function of the corresponding pK_a values for the incorporated secondary metals is supportive of our hypothesis of diminished donor power from the phenoxide ligands upon incorporation of the cations into the macrocyclic structure of **[VO]**. The total span of hyperfine coupling constants measured here (ΔA = 6 MHz from **[VO,Cs]** to **[VO,Ca]**) is commensurate with tuning of phenoxide donor ligands that bridge similarly between V and **M** in all cases; the values appear appropriate within

the spread of A_{iso} values from the literature that is more widely varying when the inner-sphere ligands are wholly substituted.[34] Finally, we confirm here that replicate measurements and simulations suggest the error on our fitted A_{iso} values is ±0.1 MHz (reported as ±1σ), suggesting that we can reliably interpret the span of values obtained for the full series of **[VO,M]** complexes (see SI, Figure S40 and Table S1).

In this work, we chose to quantify A_{iso} values through EasySpin simulation of our experimental spectroscopic data. These data were obtained in liquid solution, giving rise to spectra that could be readily compared amongst themselves. As described by Britt and co-workers[28] and studied by Cornman et al.,[38] the hyperfine coupling constant along z that is associated with the V–O_{oxo} coordinate has been found to be relatively insensitive to coordination geometry, a finding in accord with the strong, triple bond between the oxo group and vanadium that persists under most conditions. On the other hand, the equatorial contributions to hyperfine coupling (A_x and A_y) are quite sensitive to equatorial ligand donor power as well as geometric perturbations. From our X-ray crystallographic data collected on **[VO]**, **[VO,Na]**, and **[VO,Ca]**, we can observe geometric changes in the bimetallic cores of our complexes as a function of the identity of the secondary metals. In particular, the phenoxide-to-phenoxide O•••O distances (denoted $d_{O\cdots O}$ in Table 1) decrease from 2.650(2) Å for **[VO]** to 2.604(4) Å for **[VO,Na]** and 2.583(5) Å for **[VO,Ca]**. We have noted similar contractions in our prior work with heterobimetallic complexes of uranyl[26] and zinc.[39] In any case, the data described here cannot be used to distinguish between changes in ligand donor power and the associated structural changes in the heterobimetallic complexes. We note that these are synergistic changes however, and future ligand designs could in principle be used to provide more data useful for distinguishing these phenomena. Additionally, we mention that the invariance of the A_z component along the V–O_{oxo} direction is supported by our data, as

the isotropic hyperfine coupling constant values have been able to report on the donor power in the equatorial plane as a function of the identity of the incorporated secondary metal cations.

On a final note, we also compared the vibrational data on the V–O_{oxo} asymmetric stretches measured for **[VO]**, **[VO,Na]**, and **[VO,Ca]** to the V–O_{oxo} bond distances in these compounds as determined by XRD. We wished to carry out this analysis for two reasons. First, it could allow us to glean information in the context of Badger's Rule,[40] which states that the strength of a given bond (in terms of stretching frequency) is correlated with the bond length, where shorter bonds are stronger bonds. Second, this analysis could be used to bridge the gap between the spectroscopic properties of the monometallic complex **[VO]** and the heterobimetallic complexes studied here, bringing their vibrational data onto a common axis for interpretation. In accord with our expectations, we found a tight linear correlation (see SI, Figure S28) between the V–O_{oxo} bond distance and V–O_{oxo} stretching frequency, wherein the measured contraction of this bond is correlated with increased V–O_{oxo} stretching frequencies. Notably, this trend appears reliable across the monometallic and bimetallic complexes for which we have structural data, implying support for our hypothesis regarding induced diminishment of the phenoxide electron donor power to vanadium upon incorporation of the secondary cations. This is because the data would suggest that the phenoxides are best able to serve as electron donors when no secondary metal is bound in the crown-ether-like site of our complexes. This conclusion is in accord with the positive shifts in reduction potentials that we have measured for heterobimetallic uranyl complexes, in that incorporation of more effectively Lewis acidic cations (especially trivalent cations such as Y^{3+}) results in more facile reduction of U(VI) to U(V).[26]

As the vanadyl and uranyl ions have long been viewed through a common lens in light of their similar, strongly bonded terminal oxo ligands, we anticipate that the findings from this work

could be directly applicable to contexts in which the uranyl ion is modulated by the presence of secondary metal cations.[26] In this regard, the diminishment of electron donation to the uranium metal center through synergistic interactions with secondary metal cations could provide a useful approach to tuning the spectroscopic properties of this species, which dominates the speciation of uranium in most conditions and thus making uranium species rather difficult to handle. More broadly, the approach of using a paramagnetic probe to understand electronic and magnetic changes wrought by secondary metal cations appears to be a useful strategy. As the U(V) oxidation state is associated with $S = ½$ species, exploration of such effects in this oxidation state in particular could be quite useful indeed.

CONCLUSION

Spectroscopic measurements of heterobimetallic complexes using the vanadyl ion as a probe demonstrate that incorporation of secondary metal cations results in attenuated electron donor power. Use of the chemically robust vanadyl ion as a spectroscopic reporter has enabled the measurements made here, and these in turn highlight that tunable properties become uniquely accessible through incorporation of secondary metal cations; these cations can themselves display a wide range of structural properties and effective Lewis acidities, making a wide space for future explorations on this platform. The placement of two metal centers in close proximity results in electronic tuning that appears to depend on intermetallic distance as well as the effective Lewis acidity of the secondary metal cation partner. These observations highlight that both the spatial arrangement of the metals involved as well as the influence of coupling driven by

bridging ligands should be considered in future efforts aimed at generating tunable multimetallic materials.

EXPERIMENTAL SECTION

General Considerations. All manipulations were carried out in dry N_2-filled gloveboxes (Vacuum Atmospheres Co., Hawthorne, CA) or under N_2 atmosphere using standard Schlenk techniques unless otherwise noted. All solvents were of commercial grade and dried over activated alumina using a PPT Glass Contour (Nashua, NH) solvent purification system prior to use, and were stored over molecular sieves. All chemicals were from major commercial suppliers and used as received. CD_3CN was purchased from Cambridge Isotope Laboratories and dried over 3 Å molecular sieves. ^1H and ^{19}F NMR spectra were collected on 400 and 500 MHz Bruker spectrometers and referenced to the residual protio-solvent signal[41] in the case of ^1H. ^{19}F NMR spectra were referenced and reported relative to CCl_3F as an external standard following the recommended scale based on ratios of absolute frequencies (Ξ).[42,43] Chemical shifts (δ) are reported in units of ppm. UV-Vis spectra were collected with an Ocean Optics Flame spectrometer in a 1-cm path length quartz cuvette. Infrared (IR) spectra were collected under an inert atmosphere in a dry N_2-filled glovebox (Vacuum Atmospheres Co., Hawthorne, CA). Spectra were collected with a Shimadzu IRSpirit FTIR spectrometer equipped equipped with a QATR-S single-reflection attenuated total reflectance (ATR) accessory and diamond prism plate, as well as accessories for conventional transmission measurements in cell with KBr windows. Elemental analyses were performed by Midwest Microlab, Inc. (Indianapolis, IN, USA). Electron paramagnetic resonance (EPR) spectra were collected at room temperature on a Bruker

EMXplus spectrometer in quartz capillaries placed into conventional quartz EPR tubes. The concentration of analyte in each EPR sample was 10 mM.

Synthesis of [VO]. To a suspension of **[H_2,Ba]** (0.40 g, 0.46 mmol) in $CHCl_3$ prepared according to reference 18 was added an excess of guanidinium sulfate (0.49 g, 2.28 mmol) dissolved in water. The mixture was allowed to stir for 72 h, after which the organic layer was separated and concentrated to a total volume of 10-15 mL. A solution in $CHCl_3$ containing 1 equiv. of [$VO(acac)_2$] (0.12 g, 0.46 mmol) was added slowly, followed by 4 drops of triethylamine. The solution was allowed to stir at room temperature for 2 h, at which time the solution was concentrated and chilled (–20°C) overnight to encourage precipitation of the product. After chilling overnight, ice-cold ether was added dropwise to the flask and the green precipitate was isolated by vacuum filtration. Yield: 76% (0.18 mg, 0.35 mmol). Anal. Calcd for $C_{24}H_{28}N_2O_7V$ (**[VO]**): C 56.81, H 5.56, N 5.52; Found: C 54.46, H 5.56, N 5.71. Calcd for $C_{24}H_{28}N_2O_7V + H_2O$: C 54.86, H 5.76, N 5.33. This analysis is consistent with the incorporation of 1 equiv. of H_2O during sample transport and handling.

Synthesis of [VO,Na]. 1 equiv. of Na(OTf) salt (33.9 mg, 0.20 mmol) dissolved in 10 mL CH_3CN was added to a 10 mL CH_3CN solution containing **[VO]** (100 mg, 0.20 mmol). The combined solution was allowed to stir overnight. The product was then filtered and isolated by *in vacuo* solvent removal. This compound could also be isolated by vapor diffusion of diethyl ether into a concentrated CH_3CN solution, resulting in crystals that could be isolated by vacuum filtration. Yield: 89% (119 mg, 0.18 mmol). Anal. Calcd for $C_{25}H_{28}F_3N_2NaO_{10}SV$ (**[VO,Na]**): C 44.19, H 4.15, N 4.12; Found: C 41.41, H 5.32, N 5.28. Calcd for $C_{25}H_{28}F_3N_2NaO_{10}SV + 2.5$ H_2O: C 41.44, H 4.59, N 3.87. This analysis is consistent with the incorporation of 2.5 equiv. of H_2O during sample transport and handling.

Synthesis of [VO,Ca]. 1 equiv. of $Ca(OTf)_2$ salt (33 mg, 0.10 mmol) dissolved in 10 mL CH_3CN was added to a 10 mL CH_3CN solution containing **[VO]** (50 mg, 0.10 mmol). The combined solution was allowed to stir overnight. The product was then filtered and isolated by *in vacuo* solvent removal. This compound could also be isolated by vapor diffusion of diethyl ether into a concentrated CH_3CN solution, resulting in crystals that could be isolated by vacuum filtration. Yield: 92% (77 mg, 0.91 mmol). Anal. Calcd for $C_{25}H_{28}F_3CaN_2O_{10}SV$ (**[VO,Ca]**): C 36.93, H 3.34, N 3.31; Found: C 36.92, H 3.64, N 3.52.

Synthesis of [VO,Cs]. 1 equiv. of Cs(OTf) salt (56 mg, 0.20 mmol) dissolved in 10 mL CH_3CN was added to a 10 mL CH_3CN solution containing **[VO]** (100 mg, 0.20 mmol). The combined solution was allowed to stir overnight. The product was then filtered and isolated by *in vacuo* solvent removal. This compound could also be isolated by vapor diffusion of diethyl ether into a concentrated CH_3CN solution, resulting in a powder that could be isolated by vacuum filtration. Yield: 88% (137 mg, 0.17 mmol). Anal. Calcd for $C_{25}H_{28}CsF_3N_2O_{10}SV$ (**[VO,Cs]**): C 38.04, H 3.58, N 3.55; Found: C 38.35, H 4.03, N 3.63. Calcd for $C_{25}H_{28}CsF_3N_2O_{10}SV$ + 0.1 Et_2O: C 54.86, H 5.76, N 5.33. This analysis is consistent with the observation of Et_2O in the ^1H NMR spectrum of isolated **[VO,Cs]**, which was presumably incorporated during isolation of the solid compound.

***In Situ* Preparation of [VO,M] Complexes**. In a typical experiment, 1 equiv. of the desired metal triflate salt was dissolved in 10 mL of CH_3CN and added to a 10 mL solution in CH_3CN containing **[VO]** (100 mg, 0.20 mmol). The resulting homogeneous mixture was allowed to stir overnight, filtered, and used as needed for experimentation on the *in situ* produced complex.

ASSOCIATED CONTENT

Supporting Information. The following files are available free of charge.

Spectroscopic data and crystallographic details (PDF)

Cartesian coordinates for solid-state structures from XRD (XYZ)

AUTHOR INFORMATION

Corresponding Author

* To whom correspondence should be addressed. E-mail: blakemore@ku.edu. Phone: (785) 864-3019.

ACKNOWLEDGMENT

The authors thank the generous faculty of the American Crystallographic Association's Summer Course in Chemical Crystallography for helpful discussions and technical assistance with the structural data reported in this manuscript, Prof. Allen Oliver for assistance with diffraction of crystals of **[VO]** and **[VO,Na]**, Dr. Cynthia Day and Dr. Victor Day for diffraction of crystals of **[VO,Ca]**, and Sarah Neuenswander for assistance with NMR spectroscopy. This work was supported by the U.S. Department of Energy, Office of Science, Office of Basic Energy Sciences through the Early Career Research Program (DE-SC0019169). C.M.D. was supported by the Beckman Scholars Program at the University of Kansas, funded by the Arnold & Mabel Beckman Foundation.

REFERENCES

[1] (a) Horwitz, C. P.; Ciringh, Y. Synthesis and electrochemical properties of oxo-bridged manganese dimers incorporating alkali and alkaline earth cations. *Inorg. Chim. Acta* **1994,** *225*, 191-200. (b) Horwitz, C. P.; Ciringh, Y.; Weintraub, S. T. Formation pathway of a Mn(IV),Mn(IV) bis(μ-oxo) dimer that incorporates alkali and alkaline earth cations and electron transfer properties of the dimer. *Inorg. Chim. Acta* **1999,** *294*, 133-139.

[2] Kanady, J. S.; Tsui, E. Y.; Day, M. W.; Agapie, T. A Synthetic Model of the Mn3Ca Subsite of the Oxygen-Evolving Complex in Photosystem II. *Science* **2011,** *333*, 733-736.

[3] Buss, J. A.; VanderVelde, D. G.; Agapie, T. Lewis Acid Enhancement of Proton Induced CO2 Cleavage: Bond Weakening and Ligand Residence Time Effects. *J. Am. Chem. Soc.* **2018,** *140*, 10121-10125.

[4] (a) Matsunaga, S.; Shibasaki, M. Multimetallic Schiff base complexes as cooperative asymmetric catalysts. *Synthesis* **2013,** *45*, 421-437. (b) Matsunaga, S.; Shibasaki, M. Recent advances in cooperative bimetallic asymmetric catalysis: dinuclear Schiff base complexes. *Chem. Commun.* **2014,** *50*, 1044-1057.

[5] (a) Deacy, A. C.; Moreby, E.; Phanopoulos, A.; Williams, C. K. Co(III)/Alkali-Metal(I) Heterodinuclear Catalysts for the Ring-Opening Copolymerization of CO_2 and Propylene Oxide. *J. Am. Chem. Soc.* **2020,** *142*, 19150-19160. (b) Lindeboom, W.; Fraser, D. A. X.; Durr, C. B.; Williams, C. K. Heterodinuclear Zn(II), Mg(II) or Co(III) with Na(I) Catalysts for Carbon Dioxide and Cyclohexene Oxide Ring Opening Copolymerizations. *Chem. - Eur. J.* **2021,** *27*, 12224-12231.

[6] Barlow, J. M.; Ziller, J. W.; Yang, J. Y. Inhibiting the Hydrogen Evolution Reaction (HER) with Proximal Cations: A Strategy for Promoting Selective Electrocatalytic Reduction. *ACS Catal.* **2021,** *11*, 8155-8164.

[7] Tsui, E. Y.; Agapie, T. Reduction potentials of heterometallic manganese-oxido cubane complexes modulated by redox-inactive metals. *Proc. Nat. Acad. Sci. U.S.A.* **2013,** *110*, 10084-10088.

[8] (a) Reath, A. H.; Ziller, J. W.; Tsay, C.; Ryan, A. J.; Yang, J. Y. Redox Potential and Electronic Structure Effects of Proximal Nonredox Active Cations in Cobalt Schiff Base Complexes. *Inorg. Chem.* **2017,** *56*, 3713-3718. (b) Kang, K.; Fuller, J.; Reath, A. H.; Ziller, J. W.; Alexandrova, A. N.; Yang, J. Y. Installation of internal electric fields by non-redox active cations in transition metal complexes. *Chem. Sci.* **2019,** *10*, 10135-10142.

[9] Shannon, R. D. Revised effective ionic radii and systematic studies of interatomic distances in halides and chalcogenides. *Acta Cryst. A* **1976,** *32*, 751-767.

[10] Perrin, D. D. *Ionisation Constants of Inorganic Acids and Bases in Aqueous Solution*. Pergamon Press: New York, 1982; pp. 180.

[11] Fukuzumi, S.; Ohkubo, K. Quantitative evaluation of Lewis acidity of metal ions derived from the g values of ESR spectra of superoxide: metal ion complexes in relation to the promoting effects in electron transfer reactions. *Chem. - Eur. J.* **2000,** *6*, 4532-4535

[12] Gaffen, J. R.; Bentley, J. N.; Torres, L. C.; Chu, C.; Baumgartner, T.; Caputo, C. B. A Simple and Effective Method of Determining Lewis Acidity by Using Fluorescence. *Chem* **2019,** 5 (6), 1567-1583

[13] Kumar, A.; Blakemore, J. D. On the Use of Aqueous Metal-Aqua pKa Values as a Descriptor of Lewis Acidity. *Inorg. Chem.* **2021,** *60*, 1107-1115.

[14] (a) Krogman, J. P.; Foxman, B. M.; Thomas, C. M. Activation of CO_2 by a Heterobimetallic Zr/Co Complex. *J. Am. Chem. Soc.* **2011,** *133*, 14582-14585. (b) Kuppuswamy, S.; Powers, T. M.; Krogman, J. P.; Bezpalko, M. W.; Foxman, B. M.; Thomas, C. M. Vanadium–iron complexes featuring metal–metal multiple bonds. *Chem. Sci.* **2013,** *4*, 3557-3565. (c) Sharma, P.; Pahls, D. R.; Ramirez, B. L.; Lu, C. C.; Gagliardi, L. Multiple Bonds in Uranium–Transition Metal Complexes. *Inorg. Chem.* **2019,** *58*, 10139-10147.

[15] (a) Van Staveren, C. J.; Van Eerden, J.; Van Veggel, F. C. J. M.; Harkema, S.; Reinhoudt, D. N. Cocomplexation of neutral guests and electrophilic metal cations in synthetic macrocyclic hosts. *J. Am. Chem. Soc.* **1988,** *110*, 4994-5008. (b) Van Veggel, F. C. J. M.; Harkema, S.; Bos, M.; Verboom, W.; Van Staveren, C. J.; Gerritsma, G. J.; Reinhoudt, D. N. Metallomacrocycles: synthesis, x-ray structure, electrochemistry, and ESR spectroscopy of mononuclear and heterodinuclear complexes. *Inorg. Chem.* **1989,** *28*, 1133-1148.

[16] (a) Zanello, P.; Cinquantini, A.; Guerriero, P.; Tamburini, S.; Vigato, P. A. Electrochemical behavior of acyclic and macrocyclic complexes of nickel(II), copper(II) and uranyl(VI). *Inorg. Chim. Acta* **1986,** *117*, 91-96 (b) Brianese, N.; Casellato, U.; Tamburini, S.; Tomasin, P.; Vigato, P. A. Asymmetric compartmental macrocyclic ligands and related mononuclear and hetero-dinuclear complexes with d- and/or f-metal ions. *Inorg. Chim. Acta* **1999,** *293*, 178-194. (c) Vigato, P. A.; Tamburini, S. The challenge of cyclic and acyclic Schiff bases and related derivatives. *Coord. Chem. Rev.* **2004,** *248*, 1717-2128.

[17] Kumar, A.; Lionetti, D.; Day, V. W.; Blakemore, J. D. Trivalent Lewis Acidic Cations Govern the Electronic Properties and Stability of Heterobimetallic Complexes of Nickel. *Chem. – Eur. J.* **2018,** *24*, 141-149.

[18] Golwankar, R. R.; Kumar, A.; Day, V. W.; Blakemore, J. D. Revealing the Influence of Diverse Secondary Metal Cations on Redox-Active Palladium Complexes. *Chem. – Eur. J.* **2022,** *28*, e202200344.

[19] (a) Kanso, H.; Clarke, R. M.; Kochem, A.; Arora, H.; Philouze, C.; Jarjayes, O.; Storr, T.; Thomas, F. Effect of Distortions on the Geometric and Electronic Structures of One-Electron Oxidized Vanadium(IV), Copper(II), and Cobalt(II)/(III) Salen Complexes. *Inorg. Chem.* **2020,** *59*, 5133-5148. (b) Kolawole, G. A.; Patel, K. S. The stereochemistry of oxovanadium(IV) complexes derived from salicylaldehyde and polymethylenediamines. *J. Chem. Soc. Dalton Trans.* **1981,** 1241-1245.

[20] Ballhausen, C. J.; Gray, H. B. The Electronic Structure of the Vanadyl Ion. *Inorg. Chem.* **1962,** *1*, 111-122.

[21] (a) Tsuchida, E.; Yamamoto, K.; Oyaizu, K.; Iwasaki, N.; Anson, F. C. Electrochemical Investigations of the Complexes Resulting from the Acid-Promoted Deoxygenation and Dimerization of (N,N'-Ethylenebis(salicylideneaminato))oxovanadium(IV). *Inorg. Chem.* **1994,** *33*, 1056-1063. (b) Larin, G. M.; Zelentsov, V. V.; Rakitin, Y. V.; Dyatkina, M. E. EPR study of the effect of remote substituents in ligands on the nature of the metal-ligand chemical bond in vanadyl complexes. *Zh. Neorg. Khim.* **1972,** *17*, 2136-2139.

[22] Rowe, R. A.; Jones, M. M. Vanadium(IV) oxy(acetylacetonate). *Inorg. Synth.* **1957,** *5*, 113-116.

[23] Baran, E. J. Review: spectroscopic studies of oxovanadium coordination compounds. *J. Coord. Chem.* **2001,** *54*, 215-238.

[24] (a) Pedersen, C. J. Cyclic polyethers and their complexes with metal salts. *J. Am. Chem. Soc.* **1967,** *89*, 7017-7036. (b) Blakemore, J. D.; Chitta, R.; D'Souza, F. Synthesis and study of crown ether-appended boron dipyrrin chemosensors for cation detection. *Tetrahedron Letters* **2007,** *48*, 1977-1982. (c) van der Ham, A.; Hansen, T.; Lodder, G.; Codée, J. D. C.; Hamlin, T. A.; Filippov, D. V. Computational and NMR Studies on the Complexation of Lithium Ion to 8-Crown-4. *ChemPhysChem* **2019,** *20*, 2103-2109.

[25] (a) Bjorklund, J. L.; Pyrch, M. M.; Basile, M. C.; Mason, S. E.; Forbes, T. Z. Actinyl-cation interactions: experimental and theoretical assessment of $[Np(vi)O_2Cl_4]^{2-}$ and $[U(vi)O_2Cl_4]^{2-}$ systems. *Dalton Trans.* **2019,** *48*, 8861-8871. (b) Bazhina, E. S.; Aleksandrov, G. G.; Kiskin, M. A.; Efimov, N. N.; Ugolkova, E. A.; Korlyukov, A. A.; Nikitin, O. M.; Magdesieva, T. V.; Minin, V. V.; Sidorov, A. A.; Miller, J. S.; Eremenko, I. L. Synthesis, crystal structure and spin exchange coupling in polynuclear carboxylates with $\{Li_2(VO)_2\}$ metal core. *Polyhedron* **2017,** 137, 246-255. (c) Garwick, R. E.; Schreiber, E.; Brennessel, W. W.; McKone, J. R.; Matson, E. M. Surface ligands influence the selectivity of cation uptake in polyoxovanadate–alkoxide clusters. *J. Mater. Chem. A* **2022,** *10*, 12070-12078.

[26] Kumar, A.; Lionetti, D.; Day, V. W.; Blakemore, J. D. Redox-Inactive Metal Cations Modulate the Reduction Potential of the Uranyl Ion in Macrocyclic Complexes. *J. Am. Chem. Soc.* **2020,** *142*, 3032-3041.

[27] Atzori, M.; Benci, S.; Morra, E.; Tesi, L.; Chiesa, M.; Torre, R.; Sorace, L.; Sessoli, R. Structural Effects on the Spin Dynamics of Potential Molecular Qubits. *Inorg. Chem.* **2018,** *57*, 731-740.

[28] Grant, C. V.; Geiser-Bush, K. M.; Cornman, C. R.; Britt, R. D. Probing the Molecular Geometry of Five-Coordinate Vanadyl Complexes with Pulsed ENDOR. *Inorg. Chem.* **1999,** *38*, 6285-6288.

[29] Stoll, S.; Schweiger, A. EasySpin, a comprehensive software package for spectral simulation and analysis in EPR. *J. Magn. Res.* **2006,** *178*, 42-55.

[30] Weil, J. A.; Bolton, J. R. *Electron Paramagnetic Resonance: Elementary Theory and Practical Applications*. 2nd ed.; Wiley: Hoboken, NJ, 2007.

[31] (a) Crans, D. C.; Smee, J. J.; Gaidamauskas, E.; Yang, L. The Chemistry and Biochemistry of Vanadium and the Biological Activities Exerted by Vanadium Compounds. *Chem. Rev.* **2004,** *104*, 849-902. (b) Yang, X.; Wang, K.; Lu, J.; Crans, D. C. Membrane transport of vanadium compounds and the interaction with the erythrocyte membrane. *Coord. Chem. Rev.* **2003,** *237*, 103-111.

[32] Amin, S. S.; Cryer, K.; Zhang, B.; Dutta, S. K.; Eaton, S. S.; Anderson, O. P.; Miller, S. M.; Reul, B. A.; Brichard, S. M.; Crans, D. C. Chemistry and Insulin-Mimetic Properties of Bis(acetylacetonate)oxovanadium(IV) and Derivatives. *Inorg. Chem.* **2000,** *39*, 406-416.

[33] Wüthrich, K. E.S.R. (Electron Spin Resonance) Investigation of VO^{2+} Complex Compounds in Aqueous Solution. II. *Helv. Chim. Acta* **1965,** *48*, 1012-1017.

[34] Chasteen, N. D., "Vanadyl(IV) EPR spin probes. Inorganic and Biochemical Aspects," in *Biol. Magn. Reson.*; Berliner, L. J., Reuben, J., Ed.; Plenum Press: New York, 1981; Chapter 2, Vol. 3, pp. 53-119.

[35] Dickson, F. E.; Petrakis, L. Application of electron spin resonance and electronic spectroscopy to the characterization of vanadium species in petroleum fractions. *Anal. Chem.* **1974,** *46*, 1129-1130..

[36] Smith, T. S.; LoBrutto, R.; Pecoraro, V. L. Paramagnetic spectroscopy of vanadyl complexes and its applications to biological systems. *Coordination Chemistry Reviews* **2002,** 228 (1), 1-18

[37] Holyk, N. H. An Electron Paramagnetic Resonance Study of Model Oxovanadium(IV) Complexes in Aqueous Solution: Correlation of Magnetic Properties with Ligand Type and Metal Chelate Structure. M.S. Thesis, University of New Hampshire, Durham, NH, 1979.

[38] Cornman, C. R.; Geiser-Bush, K. M.; Rowley, S. P.; Boyle, P. D. Structural and Electron Paramagnetic Resonance Studies of the Square Pyramidal to Trigonal Bipyramidal Distortion of Vanadyl Complexes Containing Sterically Crowded Schiff Base Ligands. *Inorg. Chem.* **1997,** *36*, 6401-6408..

[39] Kelsey, S. R.; Kumar, A.; Oliver, A. G.; Day, V. W.; Blakemore, J. D. Promotion and Tuning of the Electrochemical Reduction of Hetero- and Homobimetallic Zinc Complexes. *ChemElectroChem* **2021,** *8*, 2792-2802.

[40] Badger, R. M. A relation between internuclear distances and bond force constants. *J. Chem. Phys.* **1934,** 2, 128-131.

[41] Fulmer, G. R.; Miller, A. J.; Sherden, N. H.; Gottlieb, H. E.; Nudelman, A.; Stoltz, B. M.; Bercaw, E.; Goldberg, K. I. NMR Chemical Shifts of Trace Impurities: Common Laboratory Solvents, Organics, and Gases in Deuterated Solvents Relevant to the Organometallic Chemist. *Organometallics.* **2010**, *29*, 2176-2179.

[42] Harris, R. K.; Becker, E. D.; Cabral De Menezes, S. M.; Goodfellow, R.; Granger, P. NMR nomenclature. Nuclear spin properties and conventions for chemical shifts (IUPAC recommendations 2001). *Pure Appl. Chem.* **2001,** *73*, 1795-1818

[43] Harris, R. K.; Becker, E. D.; Cabral De Menezes, S. M.; Granger, P.; Hoffman, R. E.; Zilm, K. W. Further conventions for NMR shielding and chemical shifts (IUPAC recommendations 2008). *Pure Appl. Chem.* **2008,** *80*, 59-84.

TOC Graphic:

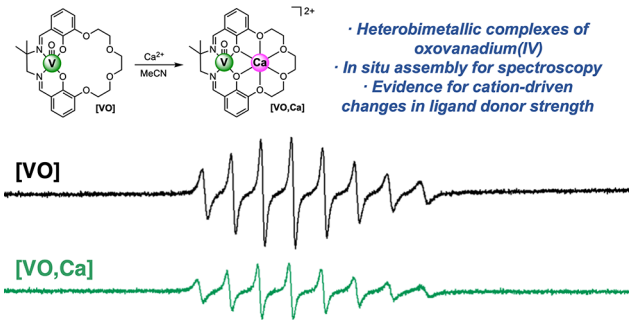

TOC Synopsis:

The oxovanadium(IV) ion has been installed in heterobimetallic complexes with secondary electropositive metal cations, and the resulting complexes have been used for spectroscopic studies. Results from infrared and EPR investigations suggest that the secondary cations serve to modulate the donor power of bridging ligands with the vanadyl center. These effects can be parametrized with a scale of effective Lewis acidity.